



MASTER THESIS
DEPARTMENT OF ATOMIC PHYSICS
LUND UNIVERSITY - FACULTY OF
ENGINEERING, LTH

Ultra-stable frequency transfer using optical fibers

- Report -

LRAP 519 (2016)

Simon Preutz

supervised by
Martin ZELAN
Lars RIPPE

help by
Sven-Christian EBENHAG

June 8, 2016

Abstract

A new era of precise time measurement came with the atomic clock. The technology is vital to navigations systems like GPS and to accurate physical measurements. Improvements in laser cooling and the development of frequency combs have combined to enable the construction of clocks using optical reference transitions, which are more stable than the Cesium standard with references in the microwave regime.

Optical fiber networks have been used to transmit stable frequencies and compare clocks but setups so far use specialized equipment. It would be advantageous to be able to use the existing optical fiber infrastructure.

In this thesis a frequency is stabilized over 80km of fiber in the lab, reaching an instability of 10^{-15} in 7000 seconds.

With a 1542.14 nm laser, frequency shifted with an acoustic optical modulator, the signal is transmitted along the fiber. A heterodyne detection scheme allows phase information to be received. A phase-locked loop regenerates the signal after the fiber and a PI controller locks the phase to a stable reference.

The maximum noise frequency that can be regulated is affected by the latency in long fibers so the delays in two pairs of fibers are measured. The 80km fiber displays a delay of 0.4ms, close to the theoretical calculated value. The 2x60km fiber that goes from SP Technical Research Institute of Sweden in Borås to Chalmers in Gothenburg display a delay of about 1ms, when the calculated value for such a distance of fiber is 0.6ms.

Further on polarization changes in the 80km fiber and the 2x60km fiber between Borås and Gothenburg is examined. The 2x60km fiber show regular variations in time at 200Hz.

Contents

Preface	iii
1 Introduction	1
1.1 Background to time measurement	1
1.2 Motivation	5
1.3 Previous work and literature	5
1.4 Objectives and challenges	6
2 Theory	7
2.1 Polarization	8
2.2 Optical fibers	7
2.3 Heterodyne detection	9
2.4 Regulation	9
2.5 Frequency stability analysis	9
3 Experimental setup and Method	11
3.1 Laser	14
3.2 AOM	14
3.3 Photo- and Phasedetection	14
3.4 Cesium reference	14
3.5 Stanford PID Regulator	15
3.6 Filters	15
4 Results and discussion	16
4.1 Minimal fiber	16
4.1.1 Initial conditions without feedback	16
4.1.2 Regulation Result	18
4.2 80km fiber	20
4.2.1 Initial condition without feedback	20
4.2.2 First regulation trial	22
4.2.3 Regulation Result	25
4.3 Chalmers	27
4.4 Polarization	28
4.5 Temperature variations	29
4.6 Latency	30
5 Conclusion and outlook	32

Preface

I want to thank Martin Zelan and Lars Rippe for guidance and supervision during the work, as well as providing helpful input along the way. I also want to thank Sven-Christian Ebenhag for insights into signal processing and electrical wiring.

I have been interested in optics and optical signals during my studies. When I began applying for a thesis it was the obvious choice. Through chance I found SP, and Martin Zelan, who supervised this project. It has been a good mix of optics and control theory that has been a privilege to work with.

1 Introduction

Correct measurements is the foundation of science. Many aspects of civilization need good measurement standards to function properly. Exchange and trade would be harder if one party considers a barrel to be 20 fingers tall and the other consider it 30 fingers tall. Since antiquity many cultures have based their measurements on seeds. China used the millet seed and Anglo-Saxon England the barely seed [1].

A seed is not optimal as a standard of measurement. Each is slightly different and can change size when dried [1]. The Roman empire created standards that partly live on to this day, like the 365 day calendar and the measure of a military pace (750mm). The metric system was designed in France in the late eighteenth century as a response to the non-existent system it had at the time. England, however, had a national system. The industrialization that was happening there required it. Assembly from parts manufactured on different locations only work if the parts are measured the same way. Since France did not have a unified system it could not compete with England. The meter was defined in 1793 and was together with the kilogram and second at the center of the metric system [1].

The International System of Units is what the metric system has evolved into. It consists of seven base units, the meter, second and kilogram being among them. These seven can be combined to express all the other units of measurements like Volt, Newton and Tesla.

Usually measurement devices change slightly over time. They can oxidize, can be heated and cooled, and may have electricity flowing through them. It can affect the measurement outcome so calibrations and comparisons to the definition are sometimes needed. Calibrations are performed by national institutes and in Sweden that is SP Technical Research Institute of Sweden. In their facilities in Borås many devices are tested and compared to standards that can be traced back to the unit definitions. There the official Swedish time is distributed.

1.1 Background to time measurement

Time was at first measured by the natural cycles in nature. Days, moon cycles and years control darkness and light and the behavior of the weather. The first and most reliable clocks in ancient history were the sundial. The oldest existing sundial is from 1500 BCE. Overcast days and nights where the weak points of a sundial, remedied by water clocks and hourglasses. However these are less stable and need to be reset according to the sundial every so often [2].

The Egyptian water clock has been around since at least 1500 BCE. It is a clay pot with a hole in the bottom that lose water at a specific rate allowing for the passage of time to be tracked by hourly markings on the pot, like in figure 2 [3].

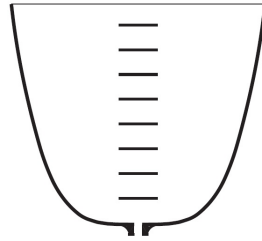


Figure 2: A water clock. The pot is filled with water and due to the shape the water will flow so that the surface decreases at the same rate during the entire time. The markings show how much time has passed [3].

Variations on this theme include the candle clock, described at around 700 CE as a candle with hourly marks. Another version, invented in the sixteenth century, was the oil clock. Instead of a candle it utilized a bottle of oil connected to an oil lamp. Hour markings were placed on the glass jar that kept the oil [3].

In 1344 the Italian astronomer Giovanni Dondi created the a mechanical clock, by causing a slowly falling weight to rotate a pin-wheel. A shaft with two paddles, connected to the top and bottom of the pin-wheel infer a periodic clockwise and counter-clockwise rotating movement to the shaft [3].

Another big step came when Galileo Galilei discovered the laws of motion governing a pendulum in 1582. A pendulum has a very regular period even while the amplitude of the oscillation decreases. However it took 55 years, until 1637, before he had made a model for a pendulum controlled clock. The principle is called pendulum escapement, allowing a wheel to turn when the pendulum swings, see figure 3 [3].

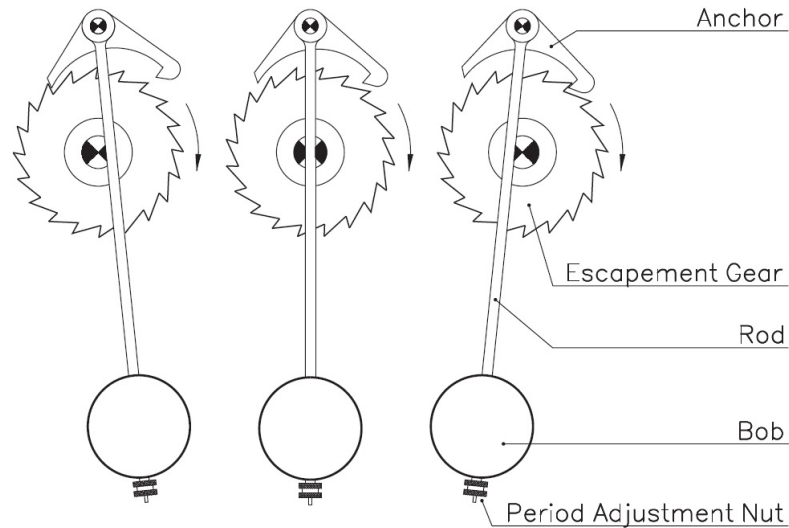


Figure 3: A pendulum clock. The pendulum swings and the anchor on top grasp and hold the wheel when the pendulum is at one side. As the pendulum swings the anchor release and the wheel turns one tick, then the anchor catches the escapement gear again. Each tick of the wheel is determined by the pendulum's period. [3]

The development in stable oscillations led Christian Huygens to invent the hairspring, or balance spring, in 1674. This is a metal spiral that twists back and forth regularly. But the oscillating frequency is not determined by gravity but on the torsion constant and the moment of inertia in the metal. With this new piece of technology the clocks could be better miniaturized, leading to today's mechanical wrist watches [3].

This improvement made it possible to create a time piece that was stable enough to bring on a ship. The crew could then use the time to figure out the longitudinal position of a ship [3]. For every 15 degrees travelled west the local time moves one hour back, so by having a clock synchronized to the time of the home port and looking at what it said when the sun was at 12 o'clock would give the longitude.

An early electrical clock uses a tuning fork, usually purposed for attuning musical instrument. The tuning fork gets a push from an electrical coil powered by a battery and a feedback circuit that cause an oscillation. The vibration of the tuning fork then pushes on a ratchet gear that drives the clock. This kind of clocks has reportedly been created with an accuracy of about 2 seconds per day [3].

To get a more accurate clock the focus had to be shifted towards crystals. Some materials are piezoelectric, that is they grow (or shrink) depending on an applied voltage. With an alternating current the crystal vibrate with a specific frequency depending on the size of the crystal and the way it is cut. When such materials are put in a controlling circuit it is possible to keep time, and in

laboratory settings to within less than a second [3].

Today the majority of our clocks are not sundials, water clocks or pendulums. Within multiple choices between oscillators, for instance pendulums, balance springs, tuning forks or crystals, the best stability can be derived from the one that vibrates the fastest. Microwave atomic clocks use an oscillation that vibrates billions of times per second and can be compared against other clocks using satellite links. [4].

The first scientific definitions of the second were based on the length of a day, one 86 400th part of the mean solar day. It had been around as a definition for a very long time but in 1967, a new definition was accepted. This was, and is, based on the stable and accurate atomic clocks that had been developed during the fifties and sixties [5].

The current second is based on the Cesium-133 microwave clock which has a frequency of 9 192 631 770 Hz. The microwave span is between 1 and 100 GHz. That corresponds to one vibration each nanosecond (10^{-9} s) to as short as each 10 picoseconds (10^{-11} s) If a pendulum swings every second then it is only possible to know the time in seconds. If a crystal oscillates a thousand times every second then it will also be possible to measure such short times. The crystal is also easier to keep stable. It is not affected by metal purity like the balance spring, nor on how it is oriented like the pendulum [3].

Increasing the frequency to the THz regime makes the radiation in an atomic clock go from microwaves to optical light. Building these optical atomic clocks have already shown better time keeping in research laboratories. The higher frequency and the capabilities to build very precise lasers might drive the accuracy and stability of the second even further [4].

The obstacles that prevented the change from microwave to optical frequencies were multifaceted. Electrical detection of the number of oscillations is one big obstacle, since electronics have a hard time detecting frequencies above GHz. Inherent noise from the movement of the atoms was also in the way. Through laser cooling it is possible to reduce the temperature of the atoms to within a millionth of a Kelvin from absolute zero [6]. This reduces the noise that come from random movement, like Doppler and collision shifts. The frequency comb solves the measurement problem. Simply put, a frequency comb is a laser system that can produce hundreds of thousands of discrete optical frequencies with a very exact difference between each frequency. By comparing the clock frequency with one of the comb teeth the measured difference frequency is low enough to count with electronics [7].

Depending on the application different methods have been used to disseminate the time. NTP, Network Time Protocol, is the internet protocol used to distribute time. It works in a hierarchy where each tier receive time from a higher tier and distribute to a lower. The top tier are the atomic clocks, and on every lower tier there are more computers and a lower accuracy. The accuracy over the internet is usually on the order of tens of microseconds [8].

To achieve a higher accuracy geostationary telecommunications satellites are utilized. The satellite links can reach timing accuracy of about 1ns in the best case [9].

1.2 Motivation

The Cesium-133 second has allowed for the creation of the Global Positioning System, GPS. It works by having atomic clocks on satellites in orbit. A GPS receiver gets a signal from a satellite and can determine their position by comparing the sending time with the receiving time. By comparing four different satellites it is possible to know the receivers relative position and then the position on earth [10].

The possible improvement optical clocks could herald are many. One example is navigational systems where better long term stability would allow for extended operations without updates and re-synchronizations [11]. An improved short term stability can improve radar techniques by achieving low phase noise microwaves [11]. Comparing ultra-stable atomic clocks allow for better tests of fundamental physical constants, for example the fine structure constant. Better clocks would yield more exact results [12]. The frequency of an atomic clock depends on the gravitational potential it is in. Further measuring a clock with a relative velocity would lead to a Doppler shift. Even so small differences as cm height difference and the cm/year velocity of the continental drifts will alter the frequency of an optical clock. With optical clocks it could be possible to measure the change in gravitational fields with more precision. [13] This would allow scientists and companies to scan the earth and detect places with different densities by comparing different fields with each other [11].

For a long time the satellites have been the best way to distribute time but recently fiber-optical time transfer has demonstrated stability at $4 * 10^{-19}$ in 100 seconds [9]. Some setups use dedicated dark fibers and have to install separate bi-directional amplifiers at each amplifier station [14] [15]. The experimental setup used in this thesis could decrease the technological cost to compare different optical oscillators against each other.

1.3 Previous work and literature

A report published in 1994 detailed the double-pass stabilization scheme that has been commonly used to transfer stable frequencies [16]. Lately, with dark fibers, special bi-directional EDFAs and single mode fibers, frequency stability have transferred over 1840km back and forth between Max-Planck-Institut für Quantenoptik (MPQ) in Garching and the Physikalisch-Technische Bundesanstalt (PTB) in Braunschweig [14]. However the availability of dark fibers and the cost of the bidirectional EDFAs puts limits on the usage of these setups right now.

A French team have used a dedicated channel in a public internet telecommunication optical fiber to transfer stable time signals over 540km [9]. They had bidirectional amplifiers and could reflect the signal back through the same fiber.

It is desired to press costs further down. Normal one-directional amplifiers and two separate fibers for the transmission back and forth may increase availability of possible transmissions routes and require less modification along the way. It has however not been shown that this concept works.

1.4 Objectives and challenges

The main focus of the thesis is to stabilize a signal over various lengths of optical fiber. The goal is to control long term frequency drift. The variations are 10 meter and 80km in the lab, and a 60km link that goes from SP Technical Research Institute of Sweden in Borås to Chalmers in Gothenburg and back again for a total length of 120km. An important point is that signals are not reflected and sent back in the same fiber like in the 1994 report [16]. Instead the signal is detected at the end. This introduces the issue that the total phase offset can't be seen as twice the one-way offset. The signal that travels to and back from Chalmers travel through different fibers in the same cable.

Since the two-way phase shift is not equal to twice the one-way shift, it is not clear what effect a stable link would have to a middle point, like at Chalmers.

The fiber is not polarization maintaining and thus the signals may become orthogonally polarized causing no interference at the detector. This will decrease the signal amplitude and effectively remove any regulation possibilities until the signal returns [17].

2 Theory

In equation 1 a wave is mathematically described where a is the amplitude, ν is the frequency, φ is the phase shift and t is the time.

$$u(t) = a * \cos(2\pi\nu t + \varphi) \quad (1)$$

Light can be described as such a wave. In figure 4 the same wave is depicted graphically. Information can be written into the wave by for instance changing the amplitude or frequency.

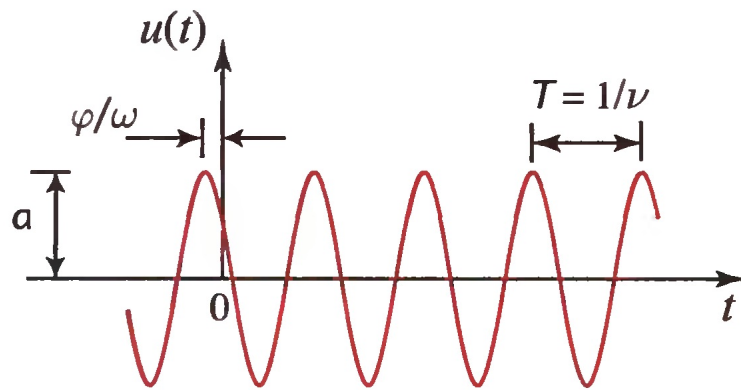
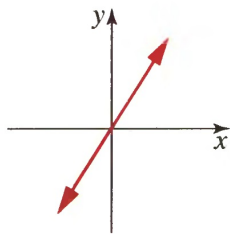


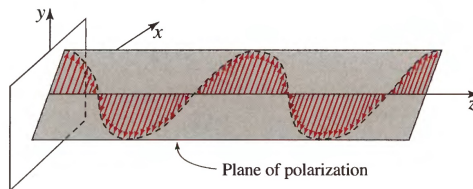
Figure 4: A mathematical description of a wave. The parameters $u(t)$ is the wave function dependent on t which is time in seconds, T is the period in seconds, ν is the frequency in Hertz, a is the amplitude, φ is the phase shift and ω is the angular frequency in radians per second [17].

2.1 Polarization

Light is electromagnetic radiation. A wave composed of two parts, the electric field vector and the magnetic field vector. These two vectors are orthogonal to each other and the direction of propagation. If the wave travels along the z axis and the electric field is oscillating along the x axis then the magnetic field is oscillating along the y axis. The electric field vector can however point in another direction as long as it is perpendicular to the direction of propagation. If the electric field oscillate in only one direction it is called linear polarization, see figure 5.



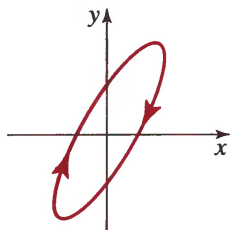
(a) The electric field oscillation seen in the x-y plane. The propagation is in the z-direction (into the page)



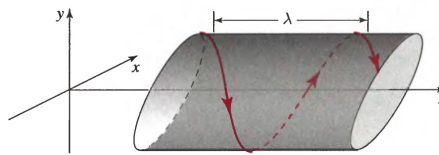
(b) Polarized radiation visualized in 3 dimensions with the electric field oscillating.

Figure 5: Two figures depicting linear polarization [17].

The polarization may also be elliptical and circular. This means that there are two perpendicular electric fields, that are phase shifted from each other like in figure 6.



(a) The electric field oscillation seen in the x-y plane. The propagation is in the z-direction.



(b) Elliptically polarized radiation visualized in 3 dimensions with the electric field oscillating.

Figure 6: Two figures depicting elliptical polarization that is not along any of the axes [17].

2.2 Optical fibers

A long fiber of quartz (silicon dioxide) is used to transmit laser radiation over long distances. The attenuation of such fibers are in the neighborhood of 0.15dB/km for the wavelength $\lambda = 1550\text{nm}$ [17]. The attenuation is strongly dependent on the wavelength of radiation passing through.

In a circular fiber two orthogonal polarizations may coexist. The two differently oriented fields have the same propagation velocities. If a single polarization is transmitted into the fiber ideally it will keep the polarization since the two orthogonal directions are not coupled. However, irregularities and strain will cause a single polarization to randomly decompose to an elliptical polarization, see figure 7 [17].

A polarization-maintaining fiber prohibits this by breaking the fiber symmetry. There are different ways to achieve this, like making an elliptical fiber or induce a stress along one direction [17].



(a) A signal passes through a non-polarization-maintaining fiber. At the end the total optical power remains the same but it is randomly distributed over the two different polarizations.



(b) When single polarized radiation instead is transmitted into polarization-maintaining fiber the power remains in the same polarization.

Figure 7: Two figures depicting the power transfer between polarizations in conventional and polarization-maintaining fiber [17].

As light travels along an optical fiber strains and vibrations induce small shifts in the material. This in turn alters the momentary phase of the light wave. In equation 1 phase is depicted as φ and when it is altered along the fiber it becomes dependent on time, $\varphi(t)$.

2.3 Heterodyne detection

Heterodyne detection is a scheme designed to allow phase information in the signal to be detected. Normally photodetectors are insensitive to the optical phase and only sensitive to the photon flux. By mixing the signal with a reference optical field, called a local oscillator, an interference pattern is created that hits the photodetector and the phase difference can be extracted, see figure 8. The incoming signal needs to have at least partly the same polarization for interference to happen and the detection scheme to work.

The intensity on the detector is given by equation 2 assuming that the signal and the local oscillator have the same polarization. I_s and I_L is the signal and local oscillator intensity, respectively. I is the intensity on the detector. $\nu_I = \nu_s - \nu_L$ is the difference frequency, φ_s is the signal phase and φ_L is the local oscillator phase.

$$I = I_s + I_L + 2\sqrt{I_s I_L} \cos[2\pi\nu_I t + (\varphi_s - \varphi_L)] \quad (2)$$

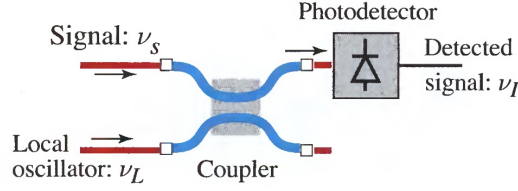


Figure 8: A setup for heterodyne detection. The coupler combines the signal and the local oscillator and allow them to interfere. ν_s is the signal frequency, ν_L is the local oscillator frequency, ν_I is the intermediate frequency [17].

2.4 Regulation

The frequency variation control is performed with a PI regulator. The control formulas in equations 3 and 4 is defined by the proportional coefficient P and the integral constant I. It is connected to the time constant and corner frequency of the feedback control.

$$\epsilon = \text{Setpoint} - \text{Measure} \quad (3)$$

$$\text{Output} = P * [\epsilon + I \int \epsilon dt] \quad (4)$$

Long fibers will cause a delay in the system. The delay limits the noise frequency that can be suppressed. Equation 5 describe the highest noise frequency that can be reduced depending on the delay [14].

$$f_{noise} < \frac{1}{2\tau} \quad (5)$$

2.5 Frequency stability analysis

The stability of the system is examined in a couple of ways. Frequency counters without dead-free measurements provide information if the frequency deviates from the reference. The counters measure the time between each cycle during the specified gate time. When the counters are dead-free each new measurement start when the last finished. Without dead-free measurement there is a small time window where the counter doesn't measure anything at all. A dead-free counter can get information about the phase stability since all measurements are correlated to the phase at the start of the measurement. Without dead-free measurement each frequency value is uncorrelated to the previous and cannot give information about phase stability.

A time interval measurement between a reference and the signal after a fiber optic cable will detect the time from a trigger point on the reference to the same trigger point on the signal, for instance a passage through zero. The time can at most become the period of the reference. If the two signals are phase-locked the time interval will be around a constant value. If they are not phase locked they will drift, and any time value is equally likely. This kind of measurement is performed to ensure that the signal passed through the fiber is phase-locked to the reference.

The overlapping Allan variance is a measure of fractional frequency fluctuations and have the advantage over normal variance that it is convergent for most noises a clock exhibit.

It is defined in equation 6, with σ is the variance, y_i is the i th of M fractional frequency values measured with the sampling interval τ_0 , with the averaging time $\tau = m * \tau_0$, where m is the averaging factor

$$\sigma_y^2(\tau) = \frac{1}{2m^2(M - 2m + 1)} \sum_{j=1}^{M-2m+1} \left\{ \sum_{i=j}^{j+m-1} [y_{i+m}] - y_i \right\}^2 \quad (6)$$

The difference between the ordinary Allan variance and the overlapping variance is that if the averaging is with sample index a through d , the next variance is calculated with sample index b through e with an overlap instead of with d through g . It utilizes all possible combinations of the data set and thus improves the confidence of the calculation [18].

In figure 9 the instability can be seen to decrease depending on the different type of noise that is prevalent. Overlapping Allan variance can not distinguish between white and flicker phase noise so the instability slope for them are equal at -1. Without dead-free measurement however, the steepest possible instability slope is $-1/2$ due to the uncorrelated frequency measurements.

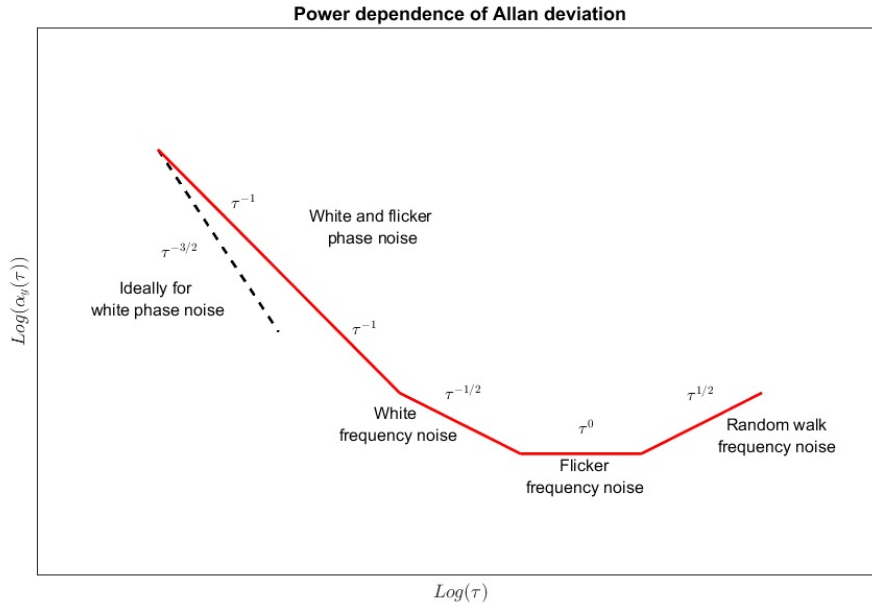


Figure 9: The power dependence of the overlapping Allan deviation on different kinds of noise. Phase noise exhibit a -1 slope, while all frequency noises have more positive slopes [18].

3 Experimental setup and Method

Phase noise along fibers can arise from for instance temperature changes, strain and vibrations. If a wave, described in equation 1, travels along a fiber then at the end the signal will have acquired a phase change that varies with time.

Comparing the changed signal to a stable reference can single out the phase change. If the phase change is slowly varying with time then the change can be compensated to a feedback to the source. In figure 10 the signal output is compared with a reference in a phase difference detector. The feedback electronics alter the output to compensate and reduce the phase difference between the signal and the reference. Thus the signal is phase locked to the reference.

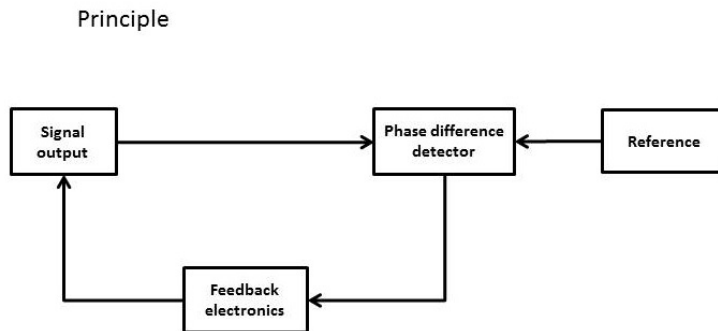


Figure 10: The principle setup. A signal output travels to a phase difference detector and compared to a reference at the same frequency as the signal. The phase difference gets supplied to the feedback electronics that alter the signal until the phase difference is zero.

To make the principle in figure 10 work for an optical signal which is transmitted in fiber optical cables several components are needed. Figure 11 describes the setup used in this thesis. A laser provides the light and an acoustic optical modulator, AOM, changes the lights frequency so that the photodetector can take advantage of heterodyne detection, see section 2.3. The detected signal is at a frequency that electronics can handle and equals the reference frequency but with the phase change that comes from the transmission in the fibers. After filtering, phase detection and PI control the feedback is sent to the AOM that adjusts the frequency shift to reduce the phase difference between the reference and the signal. Note, no stability is transferred in the experiment but it allows the setup to be evaluated with realistic noise and time delay.

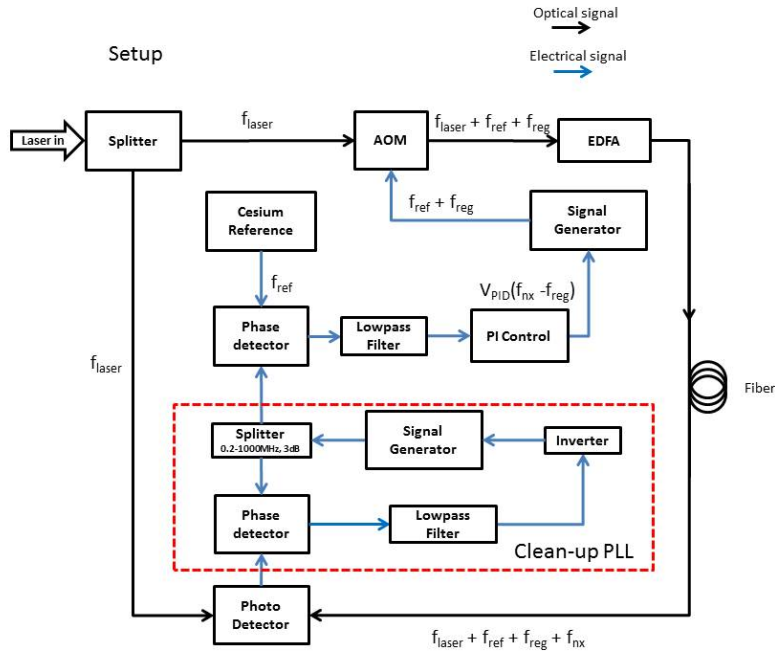


Figure 11: The main setup begins with an input laser, described in section 3.1. f_{laser} is the laser frequency, f_{ref} is the reference frequency, f_{reg} is the regulation frequency and f_{nx} is the noise. The laser light is split and then one part is sent via single mode fiber to an AOM, described in section 3.2. The shifted light that exits the signal is then amplified in an Erbium-doped fiber amplifier, EDFA, before it is sent along a desired length of fiber. In this case about 2m, 80km or 120km. Along the 120km fiber to Chalmers and back there are multiple optical amplifiers though the exact number is unknown. After transmission through the fiber the signal is beat against the original laser output in a fiber coupler. The beat signal hits the photodetector and the intermediate frequency that was shifted with the AOM is transmitted. The beat signal contains all the phase information that the signal gained during the passage in the fiber. After the photodetector a clean-up phase-locked loop, PLL, was installed when the 80km or 120km fiber was used. The signal was too noisy to send to the control system directly. And it provides support if the polarization in the fiber shifts and the signal is temporarily lost. The PLL contains a phase detector, a low-pass filter, an inverter and a signal generator. The phase detector outputs a voltage in proportion to the phase difference between the signal generator and the input signal. Through feedback the signal generator is locked in phase with the input signal except for the fast changes that the low pass filter dampens. The filtered signal from the PLL signal generator is then compared towards the Cesium reference. The phase difference is passed through an additional low pass filter and sent to the PI control unit. PI stands for proportional and integral respectively The PI controller sends a feedback signal to the signal generator that controls the AOM. Thus the shift caused by the AOM is changed to reduce the phase difference between the reference and the fiber output towards zero.

In figure 12 the actual experiment station is displayed. Some of the most important parts are highlighted by red squares. There is additional equipment to provide power, signal amplification if needed, an EDFA and an oscilloscope for checking the signal at various points.

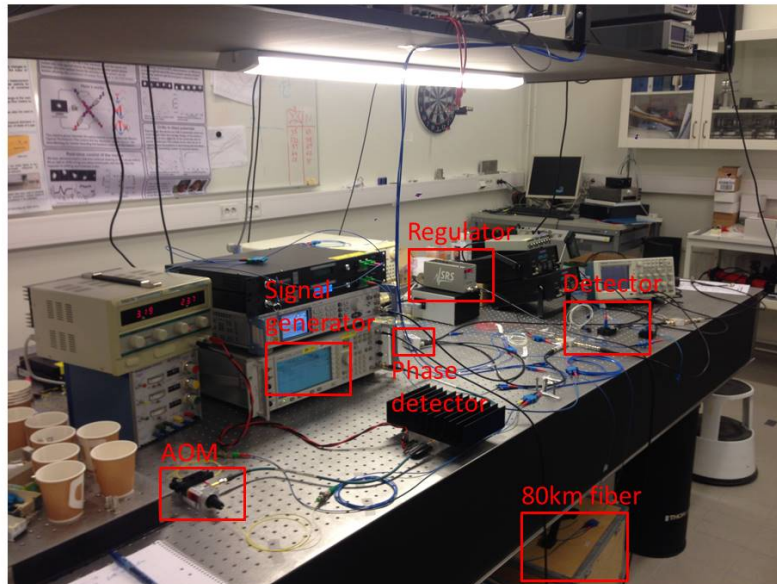


Figure 12: The experiment station. The signal generator feeds the 75MHz signal to the AOM which is then able to pass through the 80km fiber to the detector. In the phase detector a reference signal and the detected signal combine and a voltage depending on phase is transmitted to the regulator which control the AOM signal generator. The optical signal is provided from a laser, not in view, and supplied via optical fiber that travel along the ceiling.

3.1 Laser

The laser is the foundation of the system. It is an optical reference system, Menlo Systems ORS1500. It is stabilized to a cavity by the Pound-Drever-Hall technique and have a wavelength of 1542.14 nm, a linewidth of less than 1.5 Hz and the reference cavity has a finesse of more than 400000. The wavelength corresponds to a frequency of 194.53 THz. It has a linear drift of 114mHz/s due to aging of ultra-low expansion glass which the cavity spacer is made of.

3.2 AOM

The AOM comes from AAoptoelectronics AOM MT80-IIR30-Fio-2015. It shifts 1290-1650 nm light around 80 MHz (75M Hz in this case). It has singlemode fibers on the input and output, an < 3 dB insertion loss, and > 45 dB extinction ratio.

The principle is that a wave inside the crystal causes the light to scatter in different orders with different angles. In the first order the light gains a shift equal to the applied acoustic frequency.

3.3 Photo- and Phasedetection

The photodiode used is a Thorlabs PDA10CF with a detection range of 800-1700 nm. Its peak wavelength is at 1590 nm with a peak response of 1.04 A/W. Its noise equivalent power, NEP, is $1.2 * 10^{-11} W/\sqrt{Hz}$. It have a load impedance of 50 ohm, and a transimpedance gain of $5 * 10^3 V/A$.

The phase detector was a Minicircuits ZPRD-1+, 1-100 MHz, 50 ohm connections.

3.4 Cesium reference

The reference used is a Microsemi 5071A Primary Frequency Standard. It supplies a 10 MHz frequency with an instability according to figure 13. It have a typical flicker floor at $5 * 10^{-15}$.

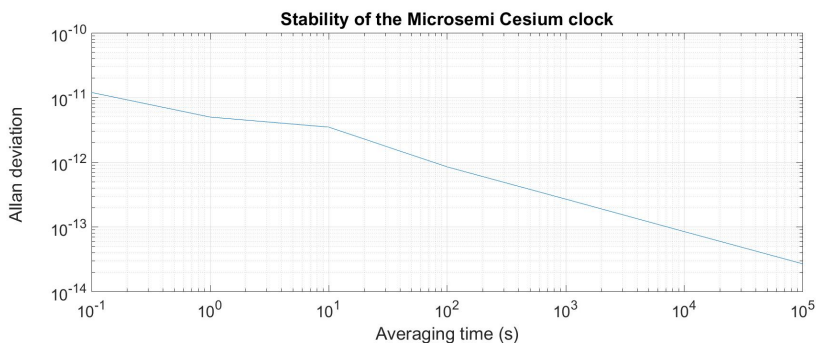


Figure 13: The Allan deviation of the reference frequency. It reaches $5 * 10^{-12}$ after 1 second. The data is taken from the device data sheet.

3.5 Stanford PID Regulator

The PID regulator used was a Stanford research systems SIM960 analog PID regulator. It has a bandwidth of 100 kHz, a 1 μ s propagation delay, and a typical input referred noise of 8 nV/\sqrt{Hz} .

The regulation parameters were based on what achieved the smallest frequency error. The 80 km regulation window was limited to low proportional and integral gain effectively making the signal unstable to fast to do a proper parameter evaluation.

The minimal fiber regulation parameters where: P=80, I=250 000 (effective time constant of 50 s) and a voltage to hertz translation of 1 kHz/V.

The 80 km fiber regulation parameters where: P=1, I=25 (effective time constant of 5 ms) and a voltage to hertz translation of 5 kHz/V.

3.6 Filters

The low pass filters in figure 11 are used to dampen fast variations. Too fast changes cannot be regulated due to delays in the fiber. The slow variations cause long term instabilities and can more easily be controlled.

Variations on the low pass range include DC-2 kHz, DC-20 kHz, DC-5 MHz and DC-11 MHz. After the photodetector a 66-78 MHz bandpass filter was used to single out the 75 MHz signal.

4 Results and discussion

With an Agilent 5320A frequency counter connected to the photodetector the frequency of the signal was measured. It counts with non-dead-free measurements so the frequency values are not correlated. A completely non-correlated measurement gives at best an instability slope of $-1/2$ while if a dead-free counter would have been used, it would be possible to get an instability slope of -1 . The data was analysed with overlapping Allan deviation, calculated on the measured fractional frequency deviation. The fractional frequency deviation is calculated by dividing the frequency deviation with the optical carrier frequency 194.53 THz. In order to confirm that the feedback worked as it was supposed the first measurements were performed on the smallest fiber length the lab supported.

4.1 Minimal fiber

Minimal fiber is in this thesis simply the shortest optical fiber needed to connect the components together. The Menlo laser is on a vibrational controlled platform a few meters from the optical bench. The rest of the equipment is on the bench. The total travel length in the fibers was less than 10 meters and the distance between the AOM and the photodetector is about 2 meters.

4.1.1 Initial conditions without feedback

Initially the frequency was measured without any feedback. In figure 14 the frequency deviation varies over short times and drifts slightly, especially in the beginning. The quick variations are due to noise in equipment and disturbances on the fiber.

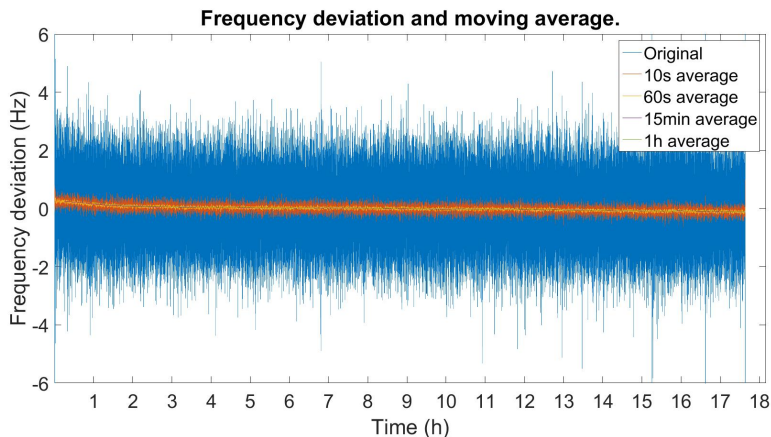


Figure 14: The initial frequency deviation of the signal through a minimal length of fiber. The intermediate frequency at 75 MHz has been removed to display the deviation. The frequency span is about 4 Hz. The measurement is performed over 18 hours with 10 samples per second.

In figure 15 the overlapping Allan deviation of the data in figure 14 is shown. The instability at short time averages first decreases and then reaches a plateau before decreasing again. The reason for this is unknown. After the initial

instability decrease the long term variations cause an increase in instability after averaging about 1000 s.

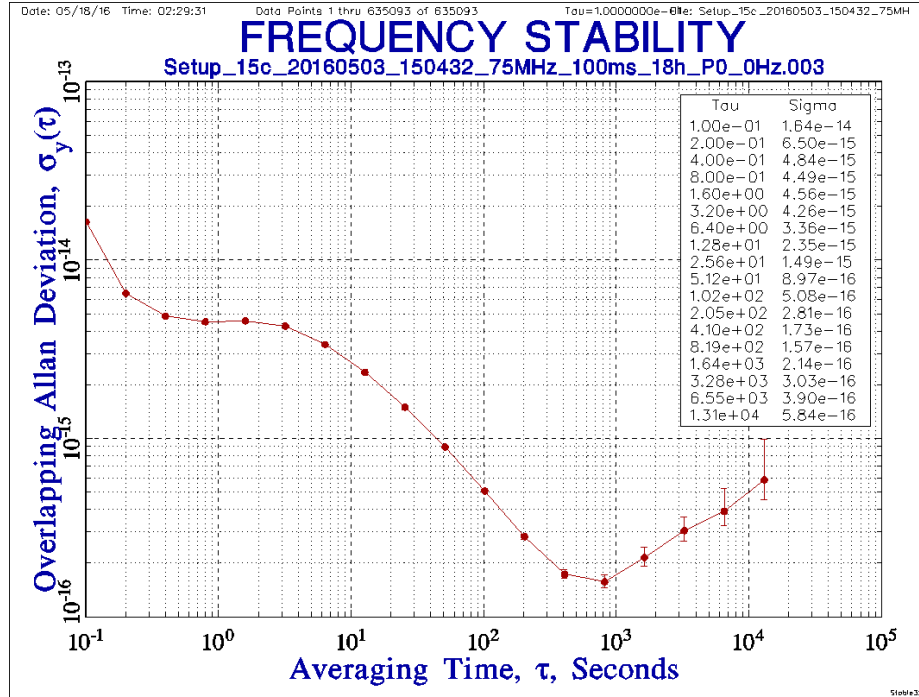


Figure 15: The instability of the initial signal through a minimal length fiber with no feedback. The measurement is performed over 18 hours with 10 samples per second. At larger time averages the uncertainty in the calculation increases as indicated by the error bars. On the right top corner the Tau is the averaging time in seconds and Sigma is the deviation.

4.1.2 Regulation Result

To control the frequency changes and long term drift a feedback loop was installed according to section 3. As seen in figure 16 the stability is improved on the short term with an decrease in frequency deviation from about 2 Hz to about 6 mHz. The resolution on the Agilent 5320A counter is up to 12 digits with a gate time of 1 second. With the signal at 75 MHz the 12th digit is 0.1 mHz. As it is described as up to 12 digits a limiting factor in this setup could be the resolution of the counters.

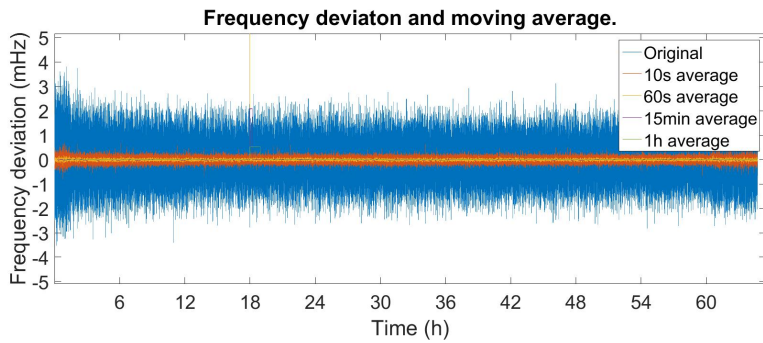


Figure 16: The regulated signal through minimal fiber, with moving averages. It is captured over 65 hours with 1 sample per second. The time scale have 6 hour increases so the axis is not cluttered. A span of about 6mHz is visible in the original signal.

In figure 17 the overlapping Allan deviation of the data in figure 16 is depicted. The instability is already at $\tau = 1$ s. lower than the unregulated signal. The plateau that the initial condition had at short times is not present at all in the regulated case. At 1000 s of averaging time the regulated signals instability keeps decreasing, a sign of a controlled signal. At 10 000 s the instability flattens but the uncertainty, in the calculations, represented by the error bars, makes it hard to properly establish.

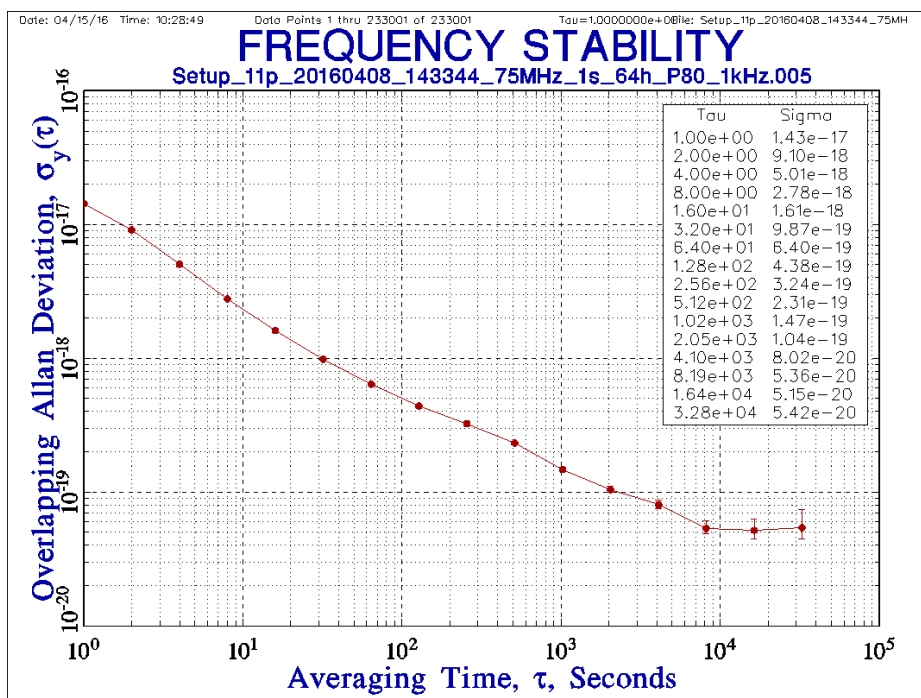


Figure 17: The frequency instability, calculated with the overlapping Allan deviation. It is captured over 65 hours with 1 sample per second. The instability decreases with a $-1/2$ slope from about $\tau = 10^2$ s to $\tau = 10^4$ s. Before $\tau = 10^2$ s the slope is slightly sharper than $-1/2$ and after $\tau = 10^4$ s the slope appears to flatten but the uncertainty, represented by the error bars, makes it hard to thoroughly establish.

4.2 80km fiber

With the minimal length fiber connection stable the next step was the 80km fiber in the lab. The fiber was in a box and connected after the AOM and EDFA. At first the setup was without feedback in order to get information about the initial conditions.

4.2.1 Initial condition without feedback

The initial condition signal with no feedback is depicted in figure 18. At the beginning and end there are more fast disturbances than during the rest of the measurement. This is quite likely due to daily activity inside and outside the lab causing disturbances. The measurement was started at 16.30 and after a few hours the fast variations decrease. After about 11.5 hours there is also some change, with an increase in both fast and slow variations. This correspond to a change in the temperature control in the lab at about 04.00 every weekday morning, see figure 29.

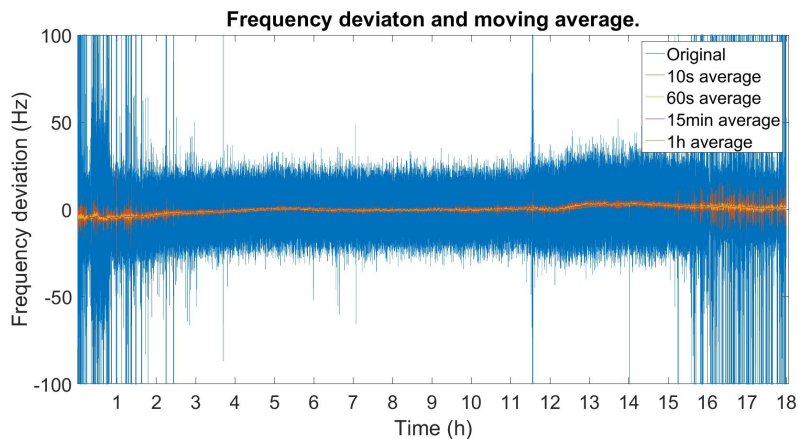


Figure 18: The frequency deviation with 80 km fiber in the lab and no regulation. It is captured over 18 hours with 10 sample per second. The 75 MHz carrier frequency has been removed centering the signal on 0 Hz. The frequency span is about 40 Hz which indicate that there is a larger phase shift in the 80 km fiber in comparison with minimal fiber. The moving average more easily show the slower variations and that the fast changes averages out.

The instability of the data in figure 18 is depicted in figure 19. At first the stability decreases with a slope lower than $-1/2$. In completely uncorrelated frequency measurements white frequency noise is the lowest slope that is measured since the phase is not taken into account. The slightly sharper slope could be an indication that the short time between each frequency measurement is quite the same which would make the measurements not completely uncorrelated. At an averaging time of about 300 seconds the instability begin to increase corresponding to the slow variations seen in figure 18.

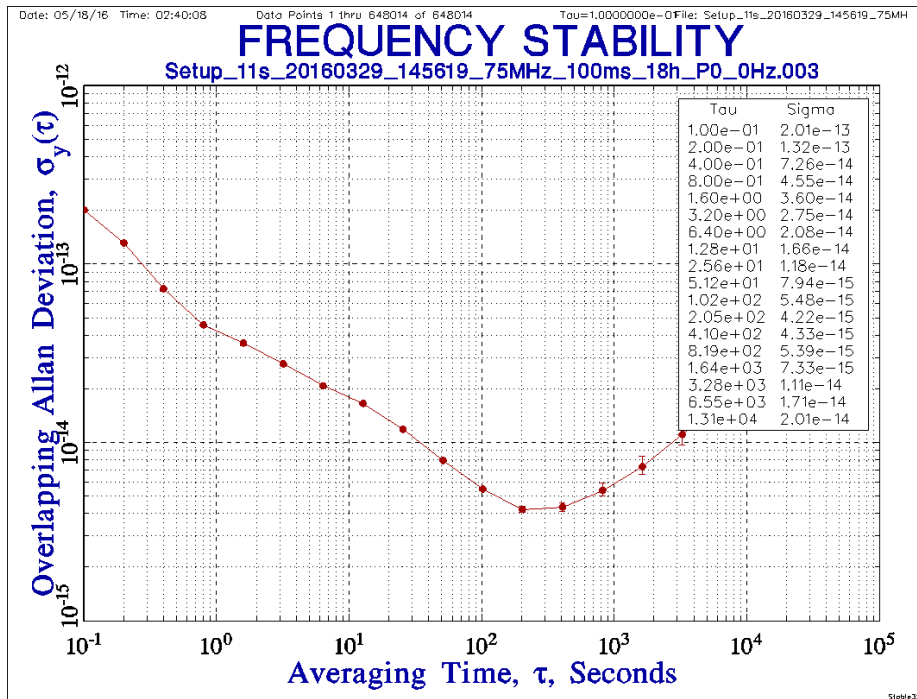


Figure 19: The frequency instability, calculated with overlapping Allan deviation. It is captured over 18 hours with 10 sample per second. Outliers have been removed prior to calculation. The instability is about 10 times larger with the 80 km fiber at an averaging time of 1 second compared with the unregulated minimal fiber. The 80 km fiber introduce larger phase shift due to its length. In the unregulated minimal fiber setup the instability, figure 15, showed a plateau up to about an averaging time of 10 seconds before it began to decrease, but here that does not show up at all.

4.2.2 First regulation trial

When the initial unregulated signal had been acquired the regulation used in the minimal length fiber was installed. However it proved not able to control the phase variations that the 80km fiber introduced. In figure 20 the frequency of the measurement with failed regulation is depicted. Some similarities with the the initial condition are the outliers in the beginning and towards the end of the measurement. After 11.5 hours there is also an outlier which corresponds to the 04.00 temperature controller change. The frequency deviation span is about 200 Hz and larger than the initial condition, due to the failed regulation increasing the variation in frequency.

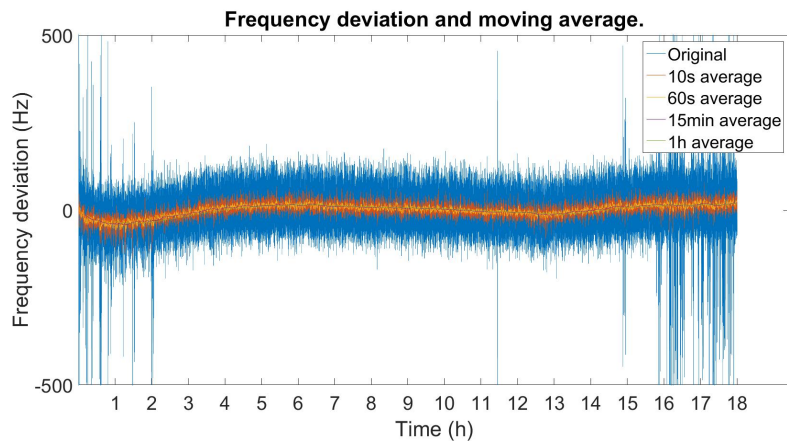


Figure 20: The frequency deviation with an unsuccessful regulation. It is captured over 18 hours with 10 sample per second. The carrier frequency at 75MHz has been removed to show the frequency deviation around 0Hz. There are outliers in the beginning and at the end and the moving averages make the slow variations more noticeable.

The instability of the failed regulation is depicted in figure 21. At short averaging times the plateau that was depicted in the unregulated minimal fiber setup is back. At longer averaging times, above 1000 seconds, the instability increases.

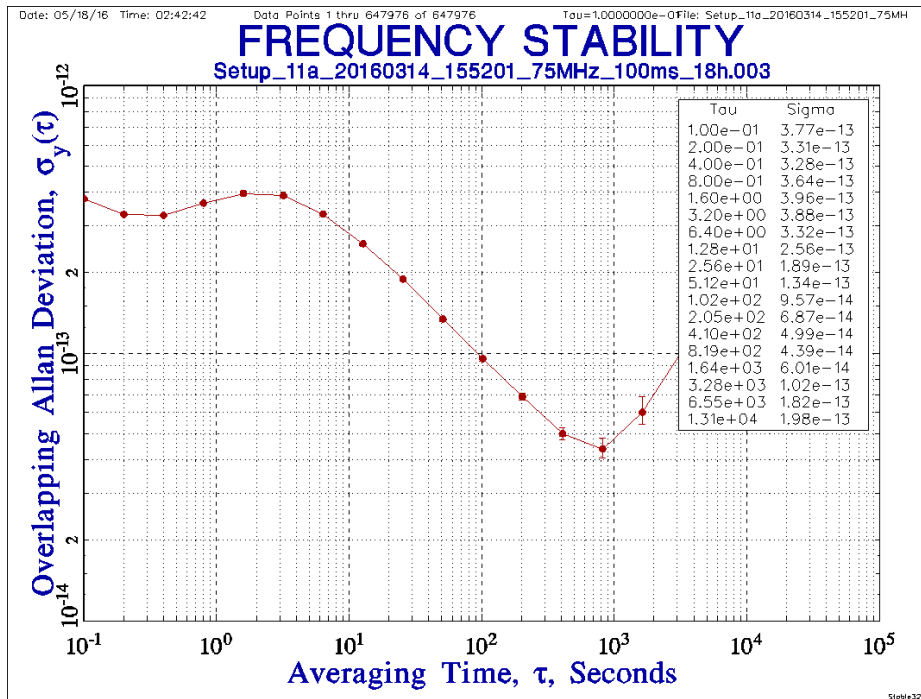


Figure 21: The frequency instability, calculated with overlapping Allan deviation. It is captured over 18 hours with 10 sample per second. Outliers have been removed prior to calculation. The unsuccessful regulation is evident in the plateau at short averaging times and the instability increase at longer averaging times.

The time interval between the reference and the signal was captured to make sure that the regulation control the phase of the signal towards the reference. If the time interval is kept close to any specific value then the control works and the phase of the signal is controlled to be around the reference phase. However the first regulation of the 80 km resulted in a time interval histogram depicted in figure 22. No interval is more likely than any other indicating no regulation.

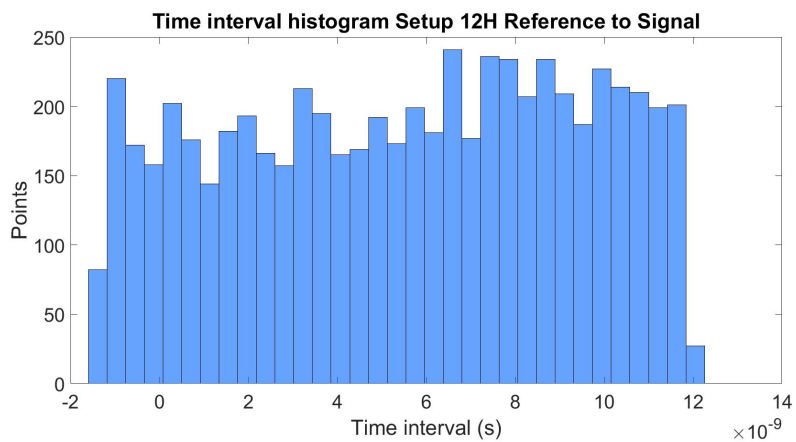


Figure 22: A histogram of a non-phaselocked signal in comparison to the reference, measured with a Pendulum CNT-90 frequency counter. The time interval in seconds on the x axis goes from -1.3 ns to 12 ns. The difference, 13.3 ns, correspond to the period of the two 75 MHz signals that are being compared.

4.2.3 Regulation Result

To enable proper feedback and control and inner clean up PLL was installed, see figure 11. It filters the fastest variations from the signal and provides a comparison that contains fewer outliers. In figure 23, the frequency deviation still has fast variations but is stable at the long term. The fastest changes to the phase may be too fast for the feedback to regulate. 80 km of fiber introduce a delay at about 0.4 ms, see figure 30 which correspond to a feedback bandwidth of 625 Hz. Any changes with components faster than 625 Hz can not be decreased with feedback.

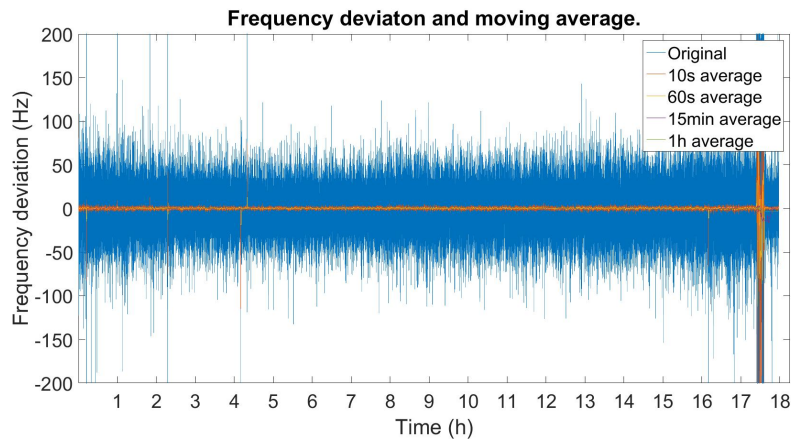


Figure 23: The frequency deviation with moving averages. It is captured over 18 hours with 10 sample per second. The average value of 75MHz was removed so the deviation is centered on 0Hz. The frequency deviation span is about 100Hz which is larger than the completely unregulated signal through 80km fiber but smaller than the failed regulation. Perhaps the control units try to regulate the fast changes as well but increase them when they can not. Over long term the frequency is stable. In the last hour the lock was lost, possibly due to construction work in the area disturbing the signal.

The instability is depicted for the first 17 hours in figure 24. The last hour was removed due to the lost control. The instability is about twice as large as the unregulated at 1 second of averaging. However the regulated signal keeps decreasing with a slope indicating white frequency noise during the entire 17 hours. When the unregulated signal instability increased at 300 seconds of averaging times the properly regulated signal keep decreasing.

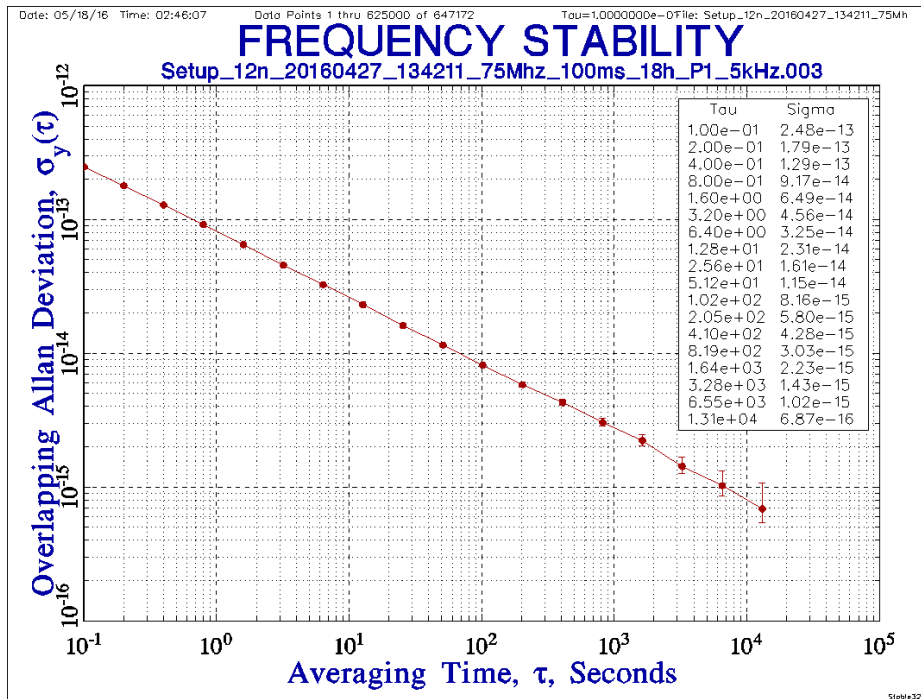


Figure 24: The output frequency instability with a regulated signal. It is captured over 18 hours with 10 sample per second. Outliers have been removed prior to calculation. The slope is stable at $-1/2$ indicating white frequency noise.

A time interval measurement between the reference and the signal was also performed and presented in figure 25. The measured interval is centred around 8 ns indicating a controlled phase-lock.

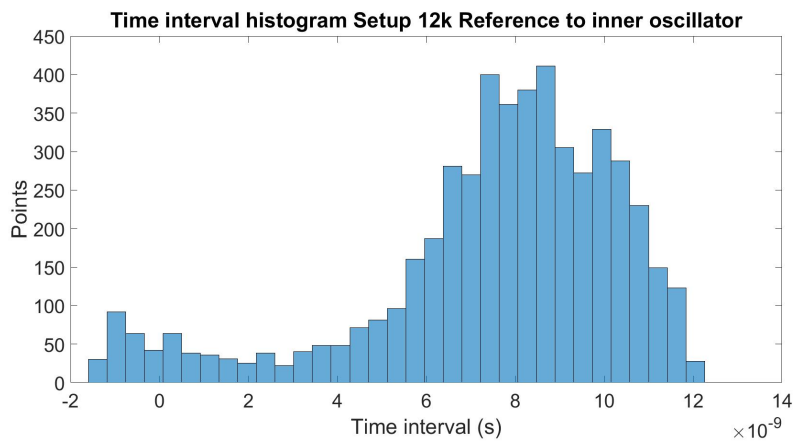


Figure 25: A histogram of a phase locked signal in comparison to the reference oscillator. A small mirroring occurs at the higher end of the period which is why there is some signal on the low side of the x-axis.

4.3 Chalmers

With the 80km fiber signal stabilized the attention turned to the 2x60km fiber from SP Technical Research Institute of Sweden to Chalmers in Gothenburg and back. However the unregulated signal is so noisy and contains so many instances where the frequency counter loses the signal that there was not enough time to properly apply feedback control to the signal. In figure 26 the initial signal is depicted. Over the 18 hour measurement the signal was not without outliers for more than 30 minutes. The outliers could be from polarization variations in the fiber. This is discussed in section 4.4.

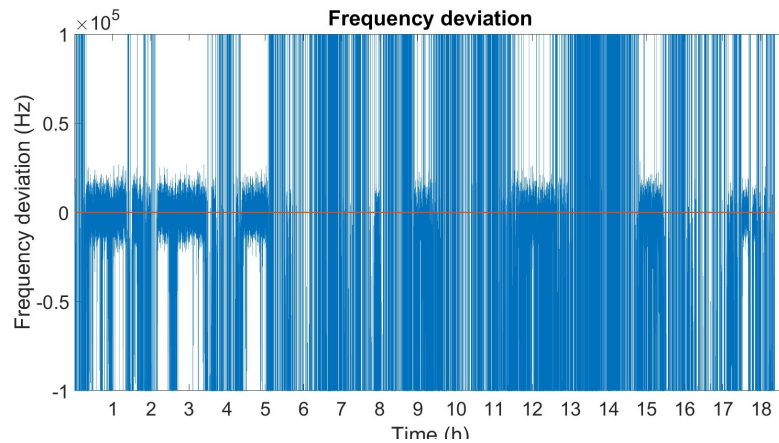


Figure 26: The frequency output after a roundtrip in the Chalmers fiber. It is captured over 18 hours with 10 sample per second. The average, 75MHz, have been removed to depict the frequency variation around 0Hz. The frequency deviation span is almost 40kHz, no considering the outliers.

4.4 Polarization

In order to further determine the cause of outliers and signal loss, especially in the fiber to Chalmers and back, two tests of the signal polarization dependency were performed. A polarization beam splitter was put after the fiber and each polarization was guided to separate photodetectors and then to a Tektronix TDS2024B oscilloscope. In figure 27 the signal has passed through the 80 km fiber. Channel 1 and 2 receive signals from the two different polarizations. The signal strength is different between the polarizations. The entire captured window represents 50 milliseconds so over short time periods the polarization in the 80km fiber does not change. As discussed in section 2.2 Optical fibers in non-polarization maintaining single mode fibers the signal can be split into two polarizations. In 2.3 Heterodyne detection it is specified that for heterodyne detection to work the two incoming signals need to have the same polarization. If the polarization varies over time the detected frequency beating will vary in amplitude.

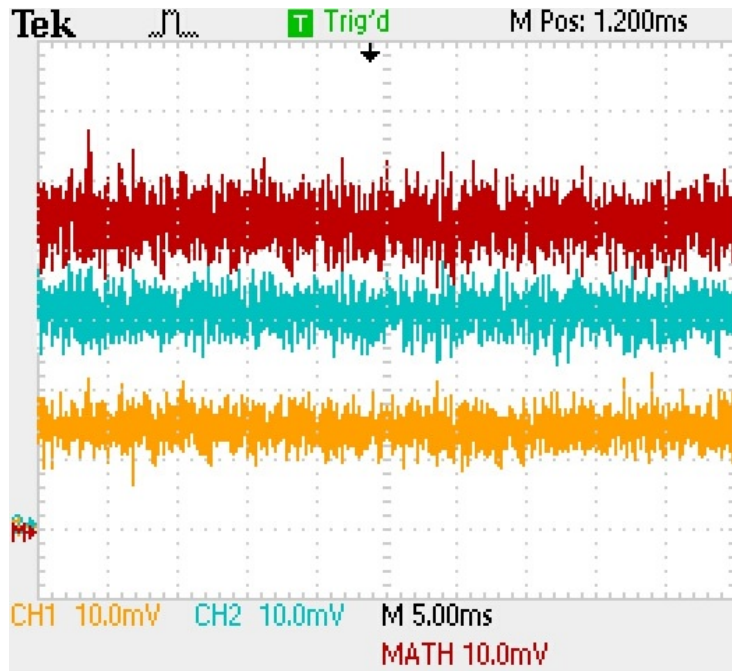


Figure 27: The detected signal through the 80 km fiber after a polarizing beam splitter. The signal to the two channels is from the two polarization states in the fiber. Math represents the sum of the two signals. During the 50 ms test the polarization doesn't vary significantly.

In figure 28 the signal has passed through the fiber to Chalmers and back before being split by the polarization beam splitter. The signal strength vary regularly in time and in sync and out of phase between the polarizations. The peaks come about every 5 ms, indicating a 200 Hz variation, but the same pattern of peaks repeat at every 20 ms, which is a 50 Hz variation. The cause of these regular polarization changes is undetermined. They do alter the signal

received at the fiber end. With a polarization that every 5 ms cause zero signal to interfere at the photodetector will cause a drop in possible regulation with that period as well. The inner PLL could help correct this as long as it can correctly lock to the incoming signal itself.

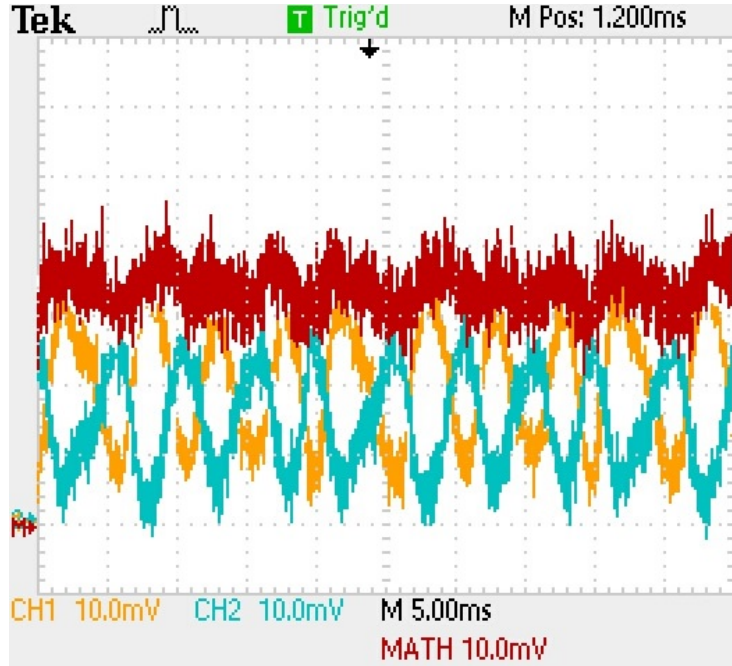


Figure 28: The signal through the Chalmers fiber after a polarizing beam splitter. The signal to the two channels is from the two polarization states in the fiber. Math represents the sum of the two signals. The polarization varies regularly in time. There is a peak in one of the channels about every 5 ms indicating 200Hz variations.

4.5 Temperature variations

The temperature in the lab is suspected to cause slower frequency fluctuations in the fiber. In order to examine the temperature profile of the lab a measurement of the temperature over a weekend was taken. It is depicted in figure 29. The temperature in the lab is 24-25 degrees Celsius during 08.30 to about 16.30. Then the temperature increases until 04.10 on workdays when the temperature start to decrease until it is fully controlled at 08.30 again. On the last day of a weekend the temperature is slowly directed to the correct range first at about 12.00 and then at 04.10 and 08.30 on the first day of work. The change in control at 04.10 is visible in some frequency measurements, figure 18 and 20.

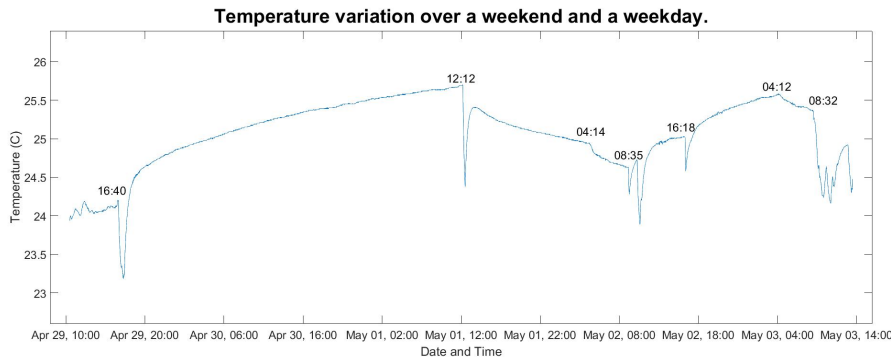


Figure 29: Temperature variation from Friday 29/4 at 10.30 to Tuesday 03/5 at 13.30. The temperature does change over time and at specific times the ventilation appear to start or be shut off. At about 16.00 the ventilation shuts down causing an increase in temperature. At around 04.00 and 08.30 the ventilation gets started again. The total variation is less than 3 degrees.

4.6 Latency

The latency, or delay, in the fibers effect the possible feedback bandwidth according to equation 5 so measurements of the latency was carried out. The 80 km fiber and the 120k m fiber to and back from Chalmers were examined using a Pendulum CNT-90 time interval counter.

In the 80 km fiber the theoretical value is 0.4 ms due to the refractive index and length of the fiber. In figure 30 the latency is shown to vary slightly over time but not regularly. The cause of this is not established. The average value of 0.387 ms is quite close to the theoretical calculation and corresponds to a maximum noise frequency that can be reduced of 1292 Hz.

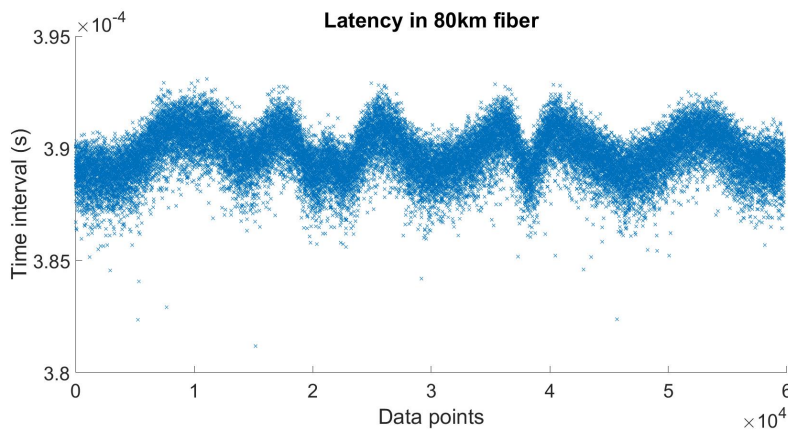


Figure 30: The transmission time in the 80 km fiber. The average value 0.387 ms corresponds quite well with a theoretical 0.4 ms. There are variations in the delay but their cause is not established.

In figure 31 the latency after travelling to and back from Chalmers is de-

picted. The theoretical value for such a long fiber is 0.6 ms but the average is 1.0546 ms. The discrepancy between the calculation and the measured value is significant but its cause is unknown. The variation is also varying in time but not as clearly. The measured delay would make the maximum noise frequency that can be reduced 474 Hz.

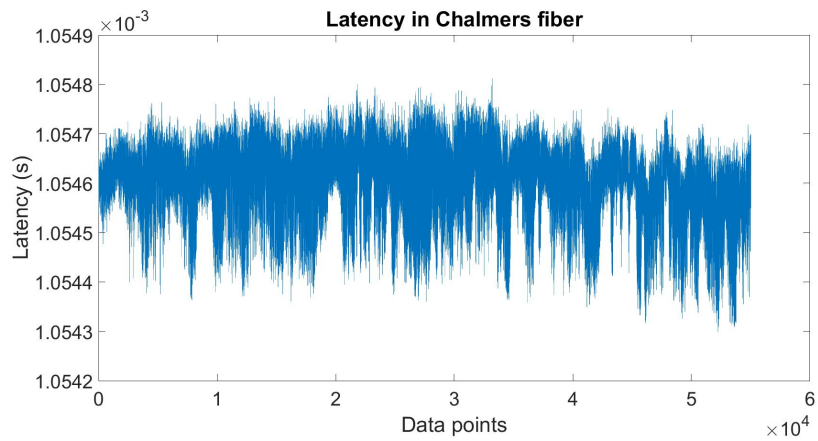


Figure 31: The transmission time in the Chalmers fiber. The calculated delay for 120 km is 0.6 ms but the measured is significantly higher for unknown reasons.

5 Conclusion and outlook

With a clean-up PLL and PI feedback control phase noise in a 80 km fiber optics cable has been reduced. Long term frequency instability has been stabilized. Latencies and polarization variations in two fibers, 80 km in the lab and 120 km from Borås to Gothenburg and back, have been characterized. Slow changes in frequency when passed through the 80 km fiber have been linked to temperature variations in the lab.

The 120km fiber was not stabilized due to time constraints. An outlook on this work is to continue experiment on the 120 km Chalmers fiber and stabilize it. Further optimization of the PI parameters might be needed and in order to keep the signal stable when the Chalmers signal is lost the clean-up PLL might need an integral control as well.

Another possible continuation is to use two fibers in the lab, stabilize the entire length and detect the signal in the middle to see if the stabilized link provides any increase in stability at that point. This is a simulation of the 120 km fiber link to and from Chalmers. As the signal does not travel in the same fiber back and forth it is not clear if the stabilization would have any benefits at a middle point, therefore the need to look at it.

References

- [1] Jeffrey H. Williams. *Defining and Measuring Nature: The make of all things*. Morgan and Claypool Publishers, 2014.
- [2] Jones E. Lawrence. *The Sundial and Geometry: An introduction for the classroom*. North American Sundial Society, 2005.
- [3] Alexius J. Hebra. *The Physics of Measurement*. SpringerWienNewYork, 2010.
- [4] A D Ludlow, T Zelevinsky, G K Campbell, S Blatt, M M Boyd, M H G de Miranda, M J Martin, J W Thomsen, S M Foreman, Jun Ye, T M Fortier, J E Stalnaker, S A Diddams, Y Le Coq, Z W Barber, N Poli, N D Lemke, K M Beck, and C W Oates. Sr lattice clock at 1×10^{-16} fractional uncertainty by remote optical evaluation with a Ca clock. *Science (New York, N.Y.)*, 319(5871):1805–8, 2008.
- [5] Barry N. Taylor and Amber Thompson. *The International System of Units (SI)*. National Institute of Standards and Technology, 2008.
- [6] William D. Phillips. Laser cooling and trapping of neutral atoms. *Reviews of Modern Physics*, 70(3):721–741, 1998.
- [7] Theodor W. Hänsch. Nobel lecture: Passion for precision. *Reviews of Modern Physics*, 78(4):1297–1309, 2006.
- [8] David L. Mills. *Computer Network Time Synchronization: The Network Time Protocol*. Taylor and Francis Group, 2006.
- [9] Olivier Lopez, Christian Chardonnet, Anne Amy-Klein, Amale Kanj, Paul Eric Pottie, Daniele Rovera, Joseph Achkar, and Giorgio Santarelli. Simultaneous remote transfer of accurate timing and optical frequency over a public fiber network. *2013 Joint European Frequency and Time Forum and International Frequency Control Symposium, EFTF/IFC 2013*, pages 474–476, 2013.
- [10] Guochang Xu. *GPS Theory, Algorithms and Applications*. Springer, 2nd edition, 2007.
- [11] Andrew D Ludlow, Martin M Boyd, Jun Ye, Ekkehard Peik, and Piet O Schmidt. Optical Atomic Clocks. *Preprint at arxiv.org/abs/1407.3493 (to appear on Rev. Mod. Phys.)*, pages 1–86, 2014.
- [12] T. M. Fortier, N. Ashby, J. C. Bergquist, M. J. Delaney, S. A. Diddams, T. P. Heavner, L. Hollberg, W. M. Itano, S. R. Jefferts, K. Kim, W. H. Oskay, T. E. Parker, J. Shirley, J. E. Stalnaker, F. Levi, and L. Lorini. Improved limits on variation of the fine structure constant and violation of Local Position Invariance. *Proceedings of the IEEE International Frequency Control Symposium and Exposition*, 070801(February):663–665, 2007.
- [13] S. Schiller, A. Görlitz, A. Nevsky, J. C J Koelemeij, A. Wicht, P. Gill, H. A. Klein, H. S. Margolis, G. Miletì, U. Sterr, F. Riehle, E. Peik, Chr Tamm, W. Ertmer, E. Rasel, V. Klein, C. Salomon, G. M. Tino, P. Lemonde,

- R. Holzwarth, and T. W. Hänsch. Optical Clocks in Space. *Nuclear Physics B - Proceedings Supplements*, 166:300–302, 2007.
- [14] S. Droste, F. Ozimek, Th Udem, K. Predehl, T. W. Hänsch, H. Schnatz, G. Grosche, and R. Holzwarth. Optical-frequency transfer over a single-span 1840 km fiber link. *Physical Review Letters*, 111(11):110801, 2013.
- [15] G Grosche, O Terra, K Predehl, R Holzwarth, B Lipphardt, F Vogt, U Sterr, and H Schnatz. Optical frequency transfer via 146 km fiber link with 10^{-19} relative accuracy. *Optics Letters*, 34(15):2270, 2009.
- [16] Long-Sheng Ma, Peter Jungner, Jun Ye, and John L Hall. Delivering the same optical frequency at two places: accurate cancellation of phase noise introduced by an optical fiber or other time-varying path. *Optics Letters*, 19(21):1777–1779, 1994.
- [17] B. E. A. Saleh and M C Teich. *Fundamentals of Photonics*. John Wiley and Sons, Inc., 2nd edition, 2007.
- [18] W.J. Riley. *Handbook of Frequency Stability Analysis*. U.S. Government printing office, 2008.